Korean J. Chem. Eng., **27**(1), 66-72 (2010)
DOI: 10.1007/s11814-009-0329-x

A kinetic model for glycerol chlorination in the presence of acetic acid catalyst

Zheng-Hong Luo†, Xiao-Zi You, and Hua-Rong Li

Department of Chemical and Biochemical Engineering, College of Chemistry and Chemical Engineering, Xiamen University, Xiamen 361005, China
(*Received 26 June 2009 • accepted 13 July 2009*)

Abstract−A kinetic model for the chlorination of glycerol with hydrochloric acid in the use of acetic acid as catalyst is presented in this study. The model is based on a comprehensive chlorination mechanism, taking the formation of 1,3-dichloro-2-propanol and 2,3-dichloro-1-propanol into account while ignoring the formation of any intermediate in the chlorination system. Simulations were carried out under different chlorination conditions to calculate the concentrations of the main chemical species in the reaction system. The validity of the model was examined via a comparison of the calculated data with the experimental data on the chlorination of glycerol with hydrochloric acid at 363-393 K. The results show the model is capable of describing the chlorination performance with good agreement with experimental data.

Key words: Glycerol, 1,3-Dichloro-2-propanol, Chlorination Kinetics, Mechanism Model

INTRODUCTION

1,3-Dichloro-2-propanol (1,3-DCP) is an intermediate for the production of epichlorohydrin (ECH, 1-chloro-2,3-epoypropane) [1], which is an important intermediate for the chemical industry [1-3]. Recently, a direct process to prepare 1,3-DCP consisting of the chlorination of glycerol (GLY) with hydrochloric acid (HCl) was developed [2,3], and the process has been widely applied in the industry. However, previous studies on the process mainly focused on the patent data and technical feasibility [1-13].

Recently, we investigated the direct preparation kinetics of 1,3-DCP from GLY with liquid HCl [14]. In our work, the direct preparation of 1,3-DCP was carried out in a batch reactor using acetic acid catalyst (HAC-catalyst) at 363-393 K. In addition, the kinetic model and its parameters of the process were also obtained, while suggested kinetics was based on a simplified mechanism of the direct preparation of 1,3-DCP from GLY, together with ignoring the formation of 2,3-Dichloro-1-propanol (2,3-DCP) [14]. Tesser et al. [15] studied the chlorination kinetics of GLY with gaseous HCl. In their work, a reaction network was suggested, together with considering the formation mechanism of 2,3-DCP (Scheme 1). Based on the network and the formation mechanism of any chemical species in the network, a consequent kinetic model using a series of ordinary differential equations (ODEs) was developed in order to quantitatively describe the chlorination kinetics at various temperatures 353-393 K.

In this work, a modified mechanism model is developed to describe the chlorination kinetics of GLY with HCl in the present of HAC. More specifically, based on the works of Luo et al. [14] and Tesser et al. [15], a comprehensive chlorination mechanism is suggested to describe the chlorination, and the mass balance equations are included to improve the performance of the kinetic model, in which the detailed deduction process of the mechanism model is also provided in this work.

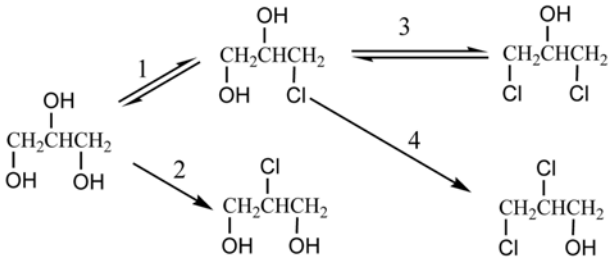

Scheme 1. The chlorination network of GLY with HCl.

EXPERIMENTAL DETAILS

Corresponding experimental details in this work are the same as those described in our previous publication [14], and the concentrations of GLY, α-MCP, β-MCP, 1,3-DCP and 2,3-DCP, *etc.* are obtained by gas chromatogram in this work.

CHLORINATION MECHANISM OF GLY IN THE PRESENCE OF HAC

The chlorination of GLY with liquid HCl, for the production of 1,3-DCP was studied in presence of HAC-catalyst. According to our previous work [14], it was found that the reaction follows the S_N2 mechanism, together with 1,3-DCP as the main product and 2,3-DCP as the byproduct. As the concentrations of 2,3-DCP is much less than that of 1,3-DCP, the formation of 2,3-DCP is ignored when considering the chlorination mechanism in Ref. [14]. In the work of Tesser and his coworkers [15], 1,3-DCP as the main product and 2,3-DCP as the byproduct were also recorded, and a complicated reaction network was suggested as Scheme 1. Based on the formation mechanism of chemical species including 2,3-DCP in the net-

†To whom correspondence should be addressed.
E-mail: luozh@xmu.edu.cn

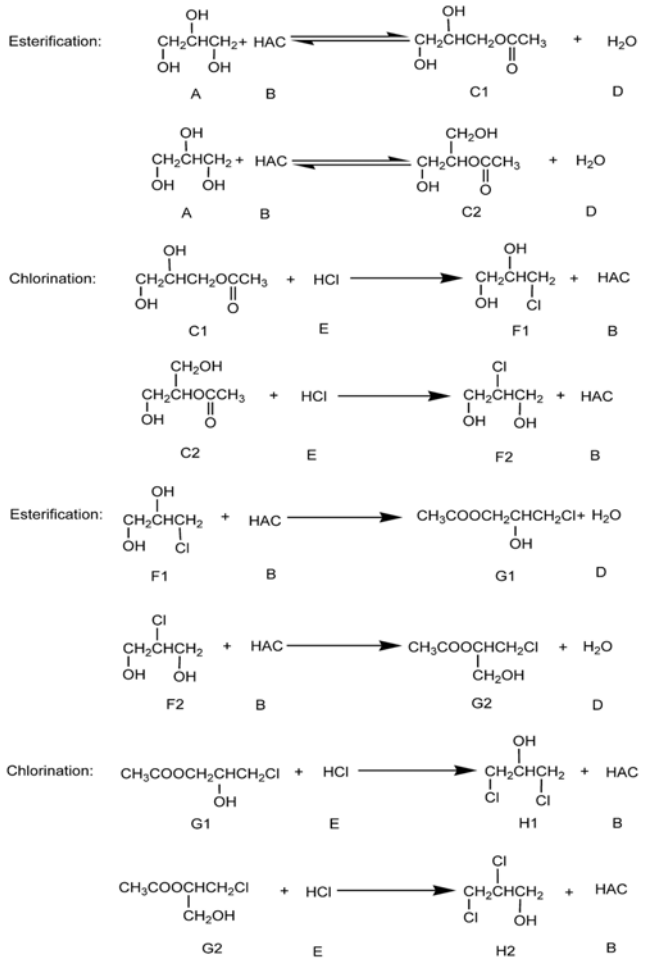

Scheme 2. The chlorination mechanism of GLY with HCl.

work, a complicated chlorination mechanism and corresponding kinetic model were derived in Ref. [15]. There we proposed a comprehensive chlorination mechanism by combining the above two original works, and the suggested comprehensive mechanism is shown in Scheme 2, where A, B, C1, C2 represent GLY, HAC, glycerol-1-acetate (1-GLYA), glycerol-2-acetate (2-GLYA) respectively, D represents water (H_2O), E represents HCl, F1 represents α-Monochlorohydrin (3-chloro-1,2-propanediol, α-MCP), F2 represents β-Monochlorohydrin (2-chloro-1,3-propanediol, β-MCP), G1 represents 3-chloropropandeiol-1-acetate (α-MCPA), G2 represents 3-chloropropandeiol-2-acetate (β-MCPA), H1 represents 1,3-DCP, H2 represents 2,3-DCP.

As a whole, the mechanism shown in Scheme 2 follows the reaction network shown in Scheme 1 as well as the S_N2 mechanism described in Ref. [14]. Therefore, the comprehensive mechanism suggested in this work considers the formation mechanism of 2,3-DCP. Furthermore, it is simpler than that shown in Ref. [15] due to considering the formation mechanism of the products (*i.e.*, 1,3-DCP and 2,3-DCP) and ignoring the formation mechanism of any intermediate in the reaction system.

KINETIC MODEL

The kinetic model of the chlorination of GLY established in this paper is based on Scheme 2 and mass balance equations for the chemical species in the chlorination system.

The following modeling assumptions are made in this paper: [3, 4,14,16] (1) the concentration of HAC is constant due to its catalytic function in the reaction system, (2) the concentration of HCl is constant and can be obtained according to its saturation in the organic phase due to its weak/difficult dissolution ability in the organic phase, (3) the concentration of H_2O is constant due to its surplus in the reaction system, and (4) the quasi-stationary-state assumption is applied. Therefore, according to the reaction steps shown in Scheme 2, the mass balance equations can be worked out.

For GLY, the following mass balance equation can be derived:

$$\frac{dc_A}{dt} = -k_1 c_A c_B + k_1' c_{C1} c_D - k_2 c_A c_B + k_2' c_{C2} c_D \quad (1)$$

Similar equations can be derived for HAC, 1-GLYA, 2-GLYA, α-MCP, β-MCP, α-MCPA, β-MCPA, 1,3-DCP and 2,3-DCP:

$$\frac{dc_B}{dt} = -k_1 c_A c_B + k_1' c_{C1} c_D - k_2 c_A c_B + k_2' c_{C2} c_D + k_3 c_{C1} c_E + k_4 c_{C2} c_E - k_5 c_{F1} c_B - k_6 c_{F1} c_B + k_7 c_{G1} c_E + k_8 c_{G2} c_E \quad (2)$$

$$\frac{dc_{C1}}{dt} = k_1 c_A c_B - k_1' c_{C1} c_D - k_3 c_{C1} c_E \quad (3)$$

$$\frac{dc_{C2}}{dt} = k_2 c_A c_B - k_2' c_{C2} c_D - k_4 c_{C2} c_E \quad (4)$$

$$\frac{dc_{F1}}{dt} = k_3 c_{C1} c_E - k_5 c_{F1} c_B \quad (5)$$

$$\frac{dc_{F2}}{dt} = k_4 c_{C2} c_E - k_6 c_{F2} c_B \quad (6)$$

$$\frac{dc_{G1}}{dt} = k_5 c_{F1} c_B - k_7 c_{G1} c_E \quad (7)$$

$$\frac{dc_{G2}}{dt} = k_6 c_{F2} c_B - k_8 c_{G2} c_E \quad (8)$$

$$\frac{dc_{H1}}{dt} = k_7 c_{G1} c_E \quad (9)$$

$$\frac{dc_{H2}}{dt} = k_8 c_{G2} c_E \quad (10)$$

According to the quasi-stationary state assumption, the following equations can be obtained:

$$\frac{dc_{C1}}{dt} = k_1 c_A c_B - k_1' c_{C1} c_D - k_3 c_{C1} c_E = 0 \quad (11)$$

$$\frac{dc_{C2}}{dt} = k_2 c_A c_B - k_2' c_{C2} c_D - k_4 c_{C2} c_E = 0 \quad (12)$$

$$\frac{dc_{G1}}{dt} = k_5 c_{F1} c_B - k_7 c_{G1} c_E = 0 \quad (13)$$

$$\frac{dc_{G2}}{dt} = k_6 c_{F2} c_B - k_8 c_{G2} c_E = 0 \quad (14)$$

Eqs. (15)-(18) can be obtained by solving Eqs. (11)-(14):

$$c_{C1} = \frac{k_1 c_A c_B}{k_1' c_D + k_3 c_E} \quad (15)$$

$$c_{C2}=\frac{k_2 c_A c_B}{k_2' c_D+k_4 c_E} \tag{16}$$

$$c_{G1}=\frac{k_5 c_{F1} c_B}{k_7 c} \tag{17}$$

$$c_{G2}=\frac{k_6 c_{F2} c_B}{k_8 c} \tag{18}$$

Therefore, we obtain the following Eqs. (19)-(23) by substituting Eqs. (11)-(18) into Eqs. (1), (5), (6), (9) and (10):

$$\frac{dc_A}{dt}=\left(-k_1 c_B-k_2 c_B+\frac{k_1 k_1' c_B c_D}{k_1' c_D+k_3 c}+\frac{k_2 k_2' c_B c_D}{k_2' c_D+k_4 c}\right)c_A=K_1 c_A \tag{19}$$

$$\frac{dc_{F1}}{dt}=\frac{k_1 k_3 c_B c_E}{k_1' c_D+k_3 c_E}c_A-k_5 c_B c_{F1}=K_2 c_A-K_3 c_{F1} \tag{20}$$

$$\frac{dc_{F2}}{dt}=\frac{k_2 k_4 c_B c_E}{k_2' c_D+k_4 c_E}c_A-k_6 c_B c_{F2}=K_4 c_A-K_5 c_{F2} \tag{21}$$

$$\frac{dc_{H1}}{dt}=k_5 c_B c_{F1}=K_3 c_{F1} \tag{22}$$

$$\frac{dc_{H2}}{dt}=k_6 c_B c_{F2}=K_5 c_{F2} \tag{23}$$

where $K_1=-k_1c_B-k_2c_B+(k_1k_1c_Bc_D/k_1c_D+k_3c_E)+(k_2k_2c_Bc_D/k_2c_D+k_4c_E)$, $K_2=(k_1k_3c_Bc_E/k_1c_D+k_3c_E)$, $K_3=k_5c_B$, $K_4=(k_2k_4c_Bc_E/k_2c_D+k_4c_E)$, $K_5=k_6c_B$, the values of c_B, c_D and c_E are constant according to the above modeling assumptions.

By integrating Eq. (19), we obtain:

$$c_A=c_{A0}e^{\left(-k_1c_B-k_2c_B+\frac{k_1k_1'c_Bc_D}{k_1'c_D+k_3c_E}+\frac{k_2k_2'c_Bc_D}{k_2'c_D+k_4c_E}\right)t}=c_{A0}e^{K_1t} \tag{24}$$

where c_{A0} is the initial value of c_A at t=0.

From Eqs. (24) & (20), (24) & (21), and K_1-K_5, we obtain:

$$\frac{dc_{F1}}{dt}+k_3c_{F1}=K_2c_{A0}e^{K_1t} \tag{25}$$

$$\frac{dc_{F2}}{dt}+k_5c_{F2}=K_4c_{A0}e^{K_1t} \tag{26}$$

Eqs. (25) and (26) are linear equations. By integrating Eqs. (25) and (26), we obtain:

$$c_{F1}e^{K_3t}=\frac{K_2c_{A0}}{K_1+K_3}e^{(K_1+K_3)t}+C_1 \tag{27}$$

$$c_{F2}e^{K_5t}=\frac{K_4c_{A0}}{K_1+K_5}e^{(K_1+K_5)t}+C_2 \tag{28}$$

At t=0, $c_{F1}=c_{F2}=0$. Therefore, we obtain: $C_1=-(K_2c_{A0}/K_1+K_3)$, $C_2=-(K_4c_{A0}/K_1+K_5)$. Accordingly, Eqs. (27) and (28) can be replaced via Eqs. (29) and (30).

$$c_{F1}=\frac{K_2c_{A0}}{K_1+K_3}(e^{K_1t}-e^{K_3t}) \tag{29}$$

$$c_{F2}=\frac{K_4c_{A0}}{K_1+K_5}(e^{K_1t}-e^{K_5t}) \tag{30}$$

From Eqs. (29) & (22), (30) & (23), and K_1-K_5, we obtain:

$$\frac{dc_{H1}}{dt}=\frac{K_2K_3c_{A0}}{K_1+K_3}(e^{K_1t}-e^{-K_3t}) \tag{31}$$

$$\frac{dc_{H2}}{dt}=\frac{K_4K_5c_{A0}}{K_1+K_5}(e^{K_1t}-e^{-K_5t}) \tag{32}$$

Eqs. (31) and (32) are separable equations. By integrating Eqs. (31) and (32), we obtain:

$$c_{H1}=\frac{K_2K_3c_{A0}}{K_1+K_3}\left(\frac{e^{K_1t}}{K_1}+\frac{e^{-K_3t}}{K_3}\right)+C_3 \tag{33}$$

$$c_{H2}=\frac{K_4K_5c_{A0}}{K_1+K_5}\left(\frac{e^{K_1t}}{K_1}+\frac{e^{-K_5t}}{K_5}\right)+C_4 \tag{34}$$

At t=0, $c_{H1}=c_{H2}=0$. Therefore, we obtain: $C_3=-(K_2K_3c_{A0}/K_1+K_3)((1/K_1)+(1/K_3))=-(K_2/K_1)c_{A0}$, $C_4=-(K_4K_5c_{A0}/K_1+K_5)((1/K_1)+(1/K_5))=-(K_4/K_1)c_{A0}$. Accordingly, Eqs. (33) and (34) can be replaced via Eqs. (35) and (36).

$$c_{H1}=\frac{K_2K_3c_{A0}}{K_1+K_3}\left(\frac{e^{K_1t}}{K_1}-\frac{e^{-K_3t}}{K_3}\right)-\frac{K_2}{K_1}c_{A0} \tag{35}$$

$$c_{H2}=\frac{K_4K_5c_{A0}}{K_1+K_5}\left(\frac{e^{K_1t}}{K_1}+\frac{e^{-K_5t}}{K_5}\right)-\frac{K_4}{K_1}c_{A0} \tag{36}$$

Eqs. (24), (29), (30), (35) and (36) will be used to describe the variation of c_A, c_{F1}, c_{F2}, c_{H1} and c_{H2} with time and temperature. In addition, the temperature dependence of the rate constants in Eqs. (24), (29), (30), (35) and (36) can be represented with Arrhenius equation and shown in Eq. (37). Hereinafter, we will examine the applicability of Eqs. (24), (29), (30), (35) and (36) by experimental data. The values of kinetic parameters can be obtained by least-square method with the data obtained experimentally.

$$k(K)=Ae^{-E_a/RT} \tag{37}$$

RESULTS AND DISCUSSION

Relating the experimental data shown in Figs. 1-5 with Eqs. (24), (29), (30), (35)-(37), we obtain the model parameters by least-square method. The obtained mechanism model parameters are listed in Table 1. The simulated data according to Eqs. (24), (29), (30), (35)

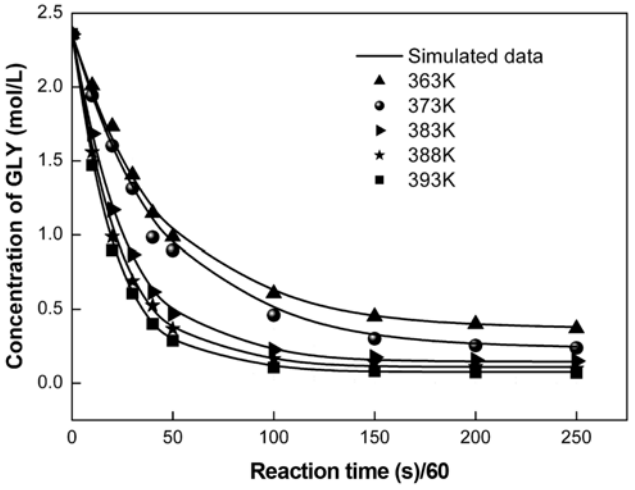

Fig. 1. Comparison between experimental and simulated data of concentration of GLY *vs.* time (Experimental conditions: c_{A0}=2.36 mol·L^{-1}; c_{B0}=0.79 mol·L^{-1}; c_{D0}=32.53 mol·L^{-1}; c_{E0}=9.42 mol·L^{-1}).

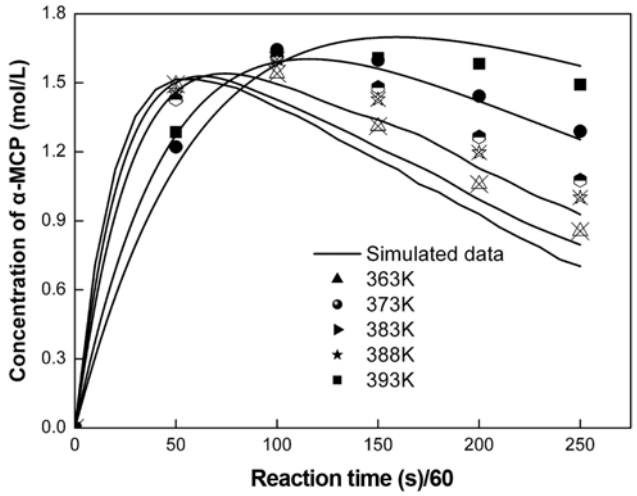

Fig. 2. Comparison between experimental and simulated data of concentration of α-MCP *vs.* time (Experimental conditions: c_{A0}=2.36 mol·L^{-1}; c_{B0}=0.79 mol·L^{-1}; c_{D0}=32.53 mol·L^{-1}; c_{E0}= 9.42 mol·L^{-1}).

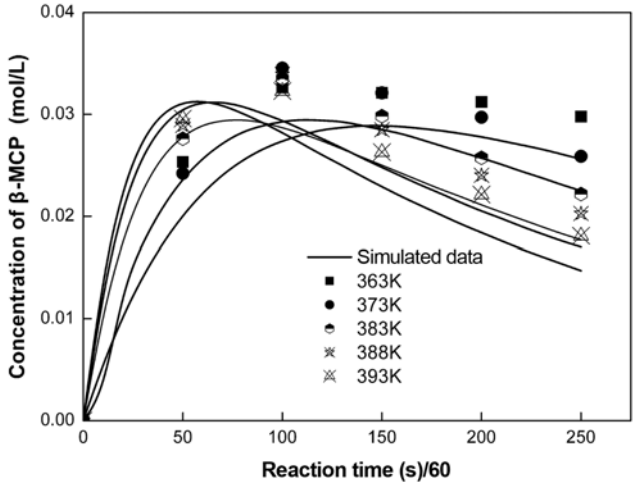

Fig. 3. Comparison between experimental and simulated data of concentration of β-MCP *vs.* time (Experimental conditions: c_{A0}=2.36 mol·L^{-1}; c_{B0}=0.79 mol·L^{-1}; c_{D0}=32.53 mol·L^{-1}; c_{E0}= 9.42 mol·L^{-1}).

and (36) by using the above model parameters are described in Figs. 1-10.

Figs. 1-10 illustrate that the comparisons between the experimental concentration and the simulated concentration. As a whole, the simulated profiles based on the improved kinetic model have good agreement with the experimental data. The average correlation coefficient of the mechanism model for all experimental data shown in Figs. 1-10 is about 0.990. The average correlation coefficient of the model suggested in Ref. [14] for corresponding experimental data exceeds 0.990. Namely, as a whole, a good agreement exists between the two model predictions and experimental measurements. Furthermore, we obtain the temperature dependence these model parameters in this present study obtained, which are shown in Figs. 11-15. The linear correlation coefficients in Figs. 11-15 all exceed 0.990.

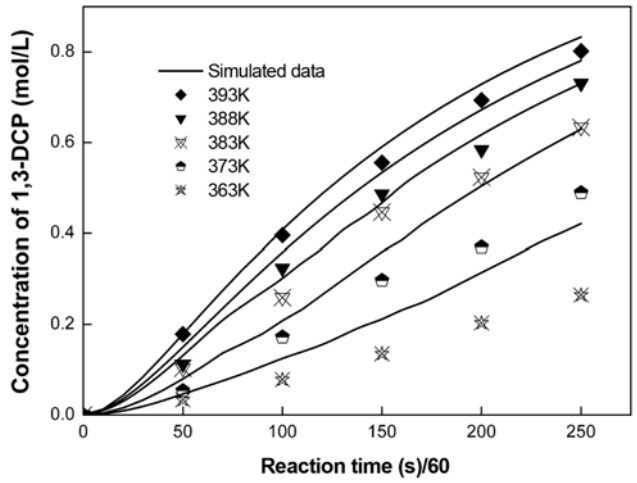

Fig. 4. Comparison between experimental and simulated data of concentration of 1,3-DCP *vs.* time (Experimental conditions: c_{A0}=2.36 mol·L^{-1}; c_{B0}=0.79 mol·L^{-1}; c_{D0}=32.53 mol·L^{-1}; c_{E0}= 9.42 mol·L^{-1}).

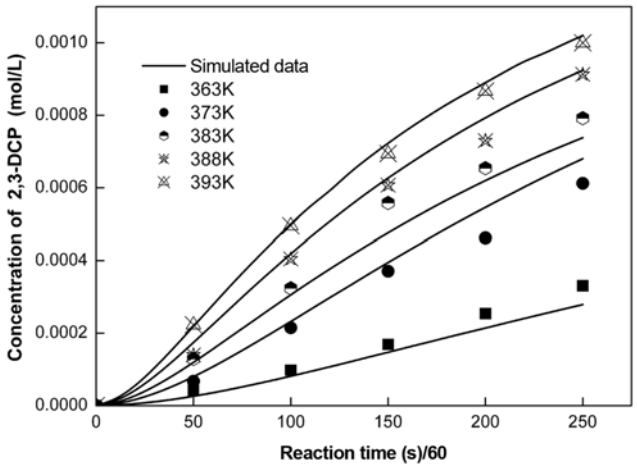

Fig. 5. Comparison between experimental and simulated data of concentration of 2,3-DCP *vs.* time (Experimental conditions: c_{A0}=2.36 mol·L^{-1}; c_{B0}=0.79 mol·L^{-1}; c_{D0}=32.53 mol·L^{-1}; c_{E0}= 9.42 mol·L^{-1}).

Table 1. The obtained kinetic model parameters by least-square method

Model parameters, (mol·L^{-1}·min^{-1})	Computational equations, $k=Ae^{(-E/RT)}$	Activation energies, (KJ·mol^{-1})
K_1	$K_1=1542.3e^{(-5702.7/T)}$	47.4
K_2	$K_2=175.6e^{(-4918.8/T)}$	40.9
K_3	$K_3=5.807e^{(-4381.2/T)}$	36.43
K_4	$K_4=40.34e^{(-7171.32/T)}$	59.6
K_5	$K_5=27.83e^{(-4950.5/T)}$	41.2

In addition, according to Figs. 1-10 and our previous study [14], we know that our previous model [15] can only predict the concentrations of GLY, α-MCP and 1,3-DCP. Besides them, the model can predict the concentration of β-MCP and 2,3-DCP. Furthermore,

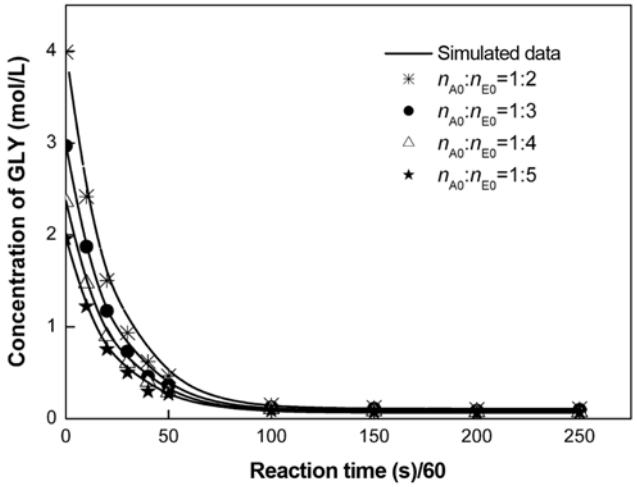

Fig. 6. Comparison between experimental and simulated data of concentration of GLY *vs.* time (Experimental conditions: c_{B0}=0.79 mol·L^{-1}; n_{E0}=4 mol; T=393 K).

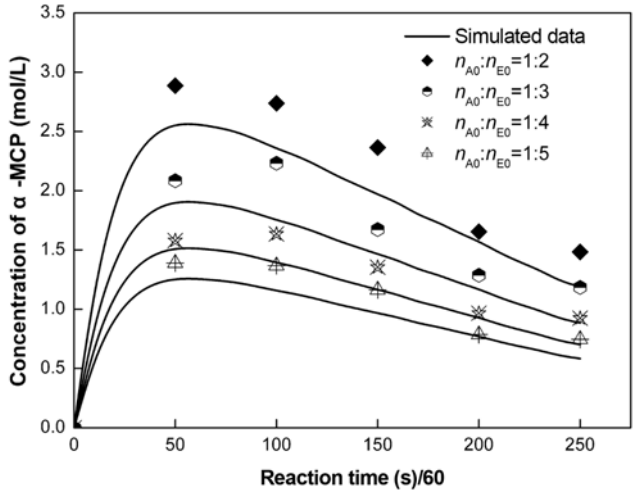

Fig. 7. Comparison between experimental and simulated data of concentration of α-MCP *vs.* time (Experimental conditions: c_{B0}=0.79 mol·L^{-1}; n_{E0}=4 mol; T=393 K).

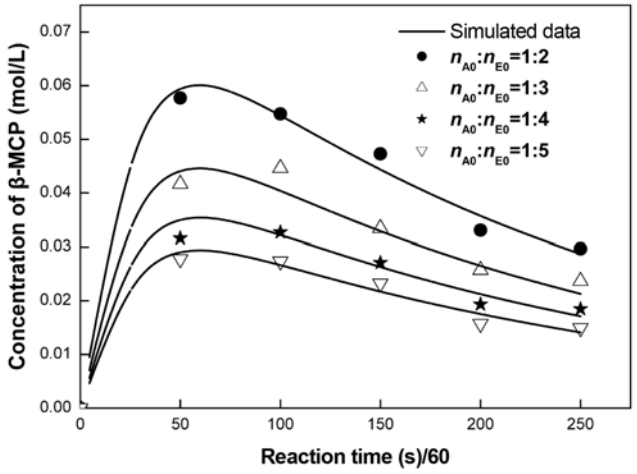

Fig. 8. Comparison between experimental and simulated data of concentration of β-MCP *vs.* time (Experimental conditions: c_{B0}=0.79 mol·L^{-1}; n_{E0}=4 mol; T=393 K).

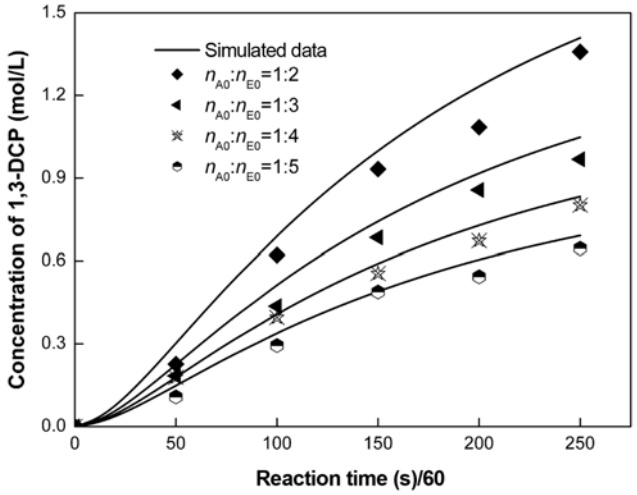

Fig. 9. Comparison between experimental and simulated data of concentration of 1,3-DCP *vs.* time (Experimental conditions: c_{B0}=0.79 mol·L^{-1}; n_{E0}=4 mol; T=393 K).

we also point out that there are different errors between the model data suggested in this work and the experimental data for different figures, as shown in Figs. 1-10. For instance, the average deviation of the mechanism model in Fig. 1 is about 3.06%, and the average deviation shown in Fig. 10 is about 4.57%.

As the model has been examined, the model and experiment are used to study the effects of the reaction temperature and the initial mole ratio of GLY and HCl in the reaction system on the chlorination kinetics. The results are also shown in Figs. 1-5 and Figs. 6-10, respectively.

Fig. 1 shows that the concentration of GLY decreases as the reaction temperature increases. In Figs. 2-3 the concentrations of α-MCP, β-MCP seem to increase in the reaction period of 0-100 min and decrease after that as the temperature increases. Figs. 4-5 show that the concentrations of 1,3-DCP and 2,3-DCP both increase with the increase of the reaction temperature. In Figs. 6-10, the simulated and experimental results all show that the concentrations of the main chemical species (*i.e.*, GLY, α-MCP, β-MCP, 1,3-DCP, 2,3-DCP) in the reaction system increase as the initial mole ratio of GLY and HCl increases. In addition, we must point out that all records by Figs. 2-10 in this study reveal that the main product and by-product of the reaction are 1,3-DCP and α-MCP, respectively. They also show that the concentration of 2,3-DCP is much less than that of 1,3-DCP, the concentration of β-MCP is also less than that of α-MCP. Even though, β-MCP still exists in the reaction system and its concentration is about 1-2 percent of that of α-MCP. Accordingly, we think that β-MCP cannot be ignored in the reaction system in the present work.

On the other hand, the concentration histories of the main chemical species in the reaction system are also described in Figs. 1-10. According to Figs. 1 and 6, we can determine that the concentration of GLY decreases to its minimum at certain time and remains

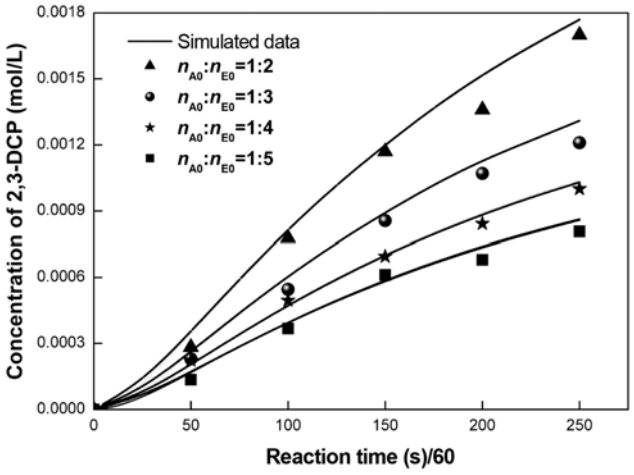

Fig. 10. Comparison between experimental and simulated data of concentration of 2,3-DCP *vs.* time (Experimental conditions: c_{B0}=0.79 mol·L^{-1}; n_{E0}=4 mol; T=393 K).

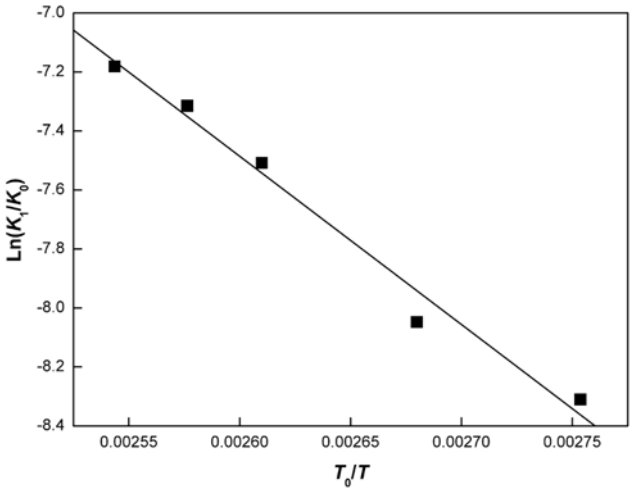

Fig. 11. Temperature-dependent reaction constant (K_1).

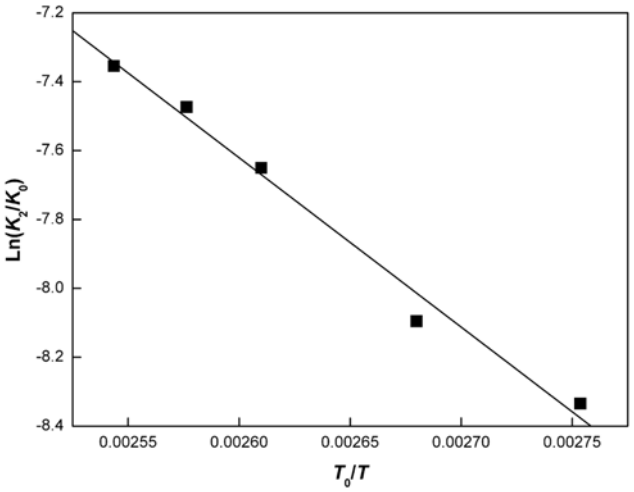

Fig. 12. Temperature-dependent reaction constant (K_2).

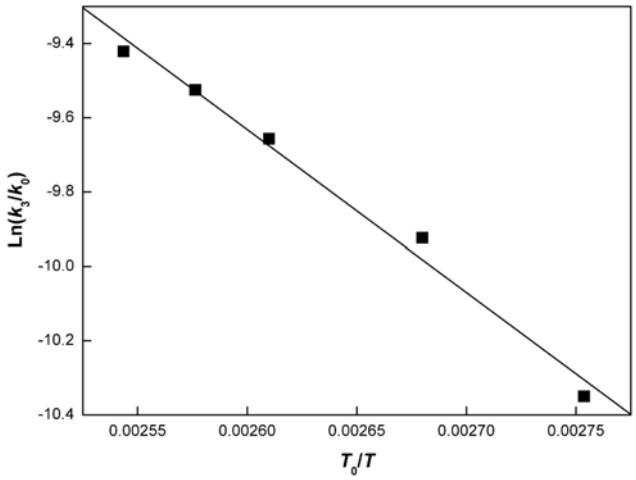

Fig. 13. Temperature-dependent reaction constant (K_3).

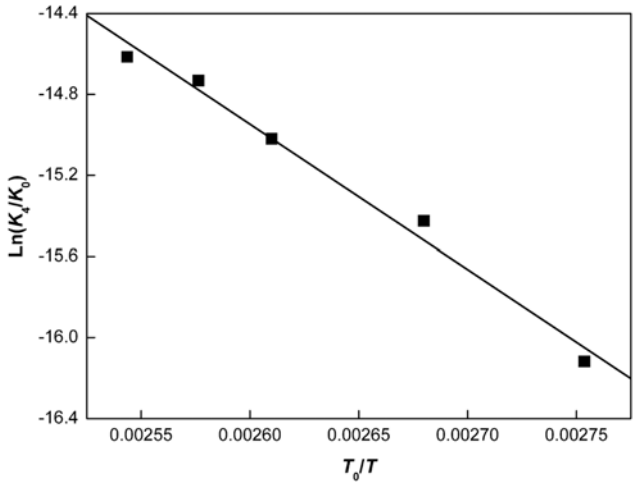

Fig. 14. Temperature-dependent reaction constant (K_4).

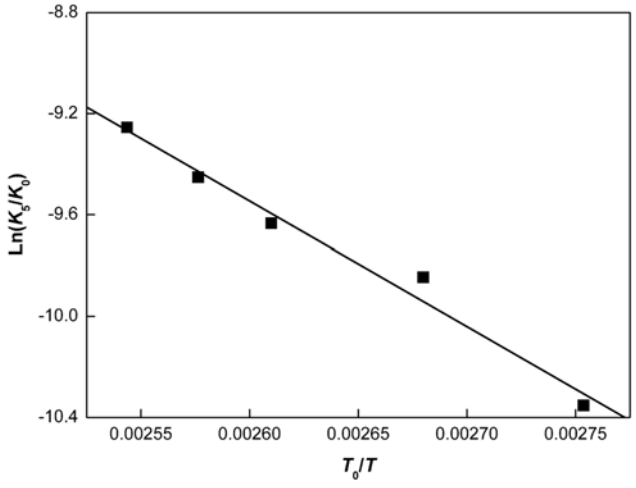

Fig. 15. Temperature-dependent reaction constant (K_5).

nearly unchanged after that with the reaction proceeding. Figs. 2-3 and 7-8 show that α-MCP and β-MCP can be produced immedi-

ately in the reaction system and their concentrations increase to their maximum at certain time and decrease after that. Furthermore, we can also obtain the concentrations of 1,3-DCP and 2,3-DCP increase during the reaction from Figs. 4-5 and 9-10.

CONCLUSIONS

The chlorination kinetics of GLY using HAC-catalyst was investigated by a mechanism model. A comprehensive chlorination mechanism and corresponding mechanism model are suggested to describe the chlorination reaction. The corresponding mechanism model, Eqs. (24), (29), (30), (35)-(37), is proposed to describe the kinetic data of the direct preparation of DCP from GLY using HAC-catalyst. The results show that the simulated data meet experimental data well. Furthermore, the results show that the improved mechanism model can predict more concentrations of species in the reaction system than our previous model [14].

ACKNOWLEDGMENTS

The authors would like to thank Yantai Wanhua Polyurethanes Co., Ltd. for financial support. The authors also thank the anonymous referees for comments on this manuscript.

NOMENCLATURE

A : collision frequency factors
c_A : concentration of GLY in reaction system [mol·L^{-1}]
c_{A0} : initial concentration of GLY in reaction system [mol·L^{-1}]
c_B : concentration of HAC in reaction system [mol·L^{-1}]
c_{B0} : initial concentration of HAC in reaction system [mol·L^{-1}]
c_{C1} : concentration of 1-GLYA in reaction system [mol·L^{-1}]
c_{C2} : concentration of 2-GLYA in reaction system [mol·L^{-1}]
c_D : concentration of H_2O in reaction system [mol·L^{-1}]
c_{D0} : initial concentration of H_2O in reaction system [mol·L^{-1}]
c_E : concentration of HCl in reaction system [mol·L^{-1}]
c_{E0} : initial concentration of HCl in reaction system [mol·L^{-1}]
c_{F1} : concentration of α-MCP in reaction system [mol·L^{-1}]
c_{F2} : concentration of β-MCP in reaction system [mol·L^{-1}]
c_{G1} : concentration of α-MCPA in reaction system [mol·L^{-1}]
c_{G2} : concentration of β-MCPA in reaction system [mol·L^{-1}]
c_{H1} : concentration of 1,3-DCP in reaction system [mol·L^{-1}]
c_{H2} : concentration of 2,3-DCP in reaction system [mol·L^{-1}]
C_1 : integral constant
C_2 : integral constant
C_3 : integral constant
C_4 : integral constant
E : activation energies [KJ·mol^{-1}]
h_μ : total number of reactant molecule of reaction μ
k_1, k'_1, k_2, k'_2, k_3, k_4, k_5, k_6, k_7 and k_8 : reaction rate constants [mol·L^{-1}·s^{-1}]
K_0 : reaction rate constant [1 mol·L^{-1}·s^{-1}]
K_1, K_2, K_3, K_4 and K_5 : model parameters for Eqs. (24)-(28) [mol·L^{-1}·s^{-1}]
n_{A0} : initial mole number of GLY in reaction system [mol]
n_{E0} : initial mole number of HCl in reaction system [mol]
R : the ideal gas constant [8.314 J·mol^{-1}·K^{-1}]
t : reaction time [s]
T : absolute temperature [K]
T_0 : absolute temperature [1 K]

REFERENCES

1. H. L. Horsley, *Encyclopedia of chemical technology*, 3th ed., Wiley, Hoboken, NJ, 595 (1965).
2. L. Ma, J. W. Zhu, X. Q. Yuan and Q. Yue, *Trans IChemE, Part A, Chem. Eng. Res. Des.*, **85**, 1580 (2007).
3. S. Carrà, E. Santacesarla and M. Morbldlll, *Ind. Eng. Chem. Process Des. Dev.*, **18**, 424 (1979).
4. L. L. Wang, Y. M. Liu and W. Xie, *J. Catal.*, **246**, 205 (2007).
5. S. H. Lee, D. R. Park, H. Kim, J. Lee, J. C. Jung, S. Y. Woo, W. S. Song, M. S. Kwon and I. K. Song, *Catal. Com.*, **9**, 1920 (2008).
6. W. Xie, H. Peng and L. Chen, *Appl. Catal. A-Gen.*, **300**, 67 (2006).
7. C. S. Macleod, A. P. Harvey, A. F. Lee and K. Wilson, *Chem. Eng. J.*, **135**, 63 (2008).
8. P. Krafft, P. Gilbeau and D. Balthasart, *Crude glycerol-based product, process for its purification and its use in the manufacture of dichloropropanol*, PCT Patent WO/2007/144335 (2007).
9. P. Gilbeau and P. Krafft, *Producing chlorinated organic compounds e.g. dichloropropanol involves using glycerol obtained from renewable raw materials, as a starting product*, FR Patent FR2868419 (2005).
10. P. Krafft, P. Gilbeau, B. Gosselin and S. Claessens, *Process for producing dichloropropanol from glycerol, the glycerol coming eventually from the conversion of animal fats in the manufacture of biodiesel*, PCT Patent WO2005/054167 A1 (2005).
11. P. Kubicek, P. Sladek and I. Buricova, *Method of preparing dichloroproanols from glycerine*, PCT Patent WO2005/021476 A1 (2005).
12. D. J. Schreck, W. J. Kruper, R. D. Varjian, M. E. Jones, R. M. Campbell, K. Kearns, B. D. Hook, J. R. Briggs and J. G. Hippler, *Conversion of a multihydroxylated-aliphatic hydrocarbon or ester thereof to a chlorohydrin*, PCT Patent WO2006/020234 A1 (2006).
13. P. Krafft, C. Franck, I. D. Andolenko and R. Veyrac, *Process for the manufacture of dichloropropanol by chlorination of glycerol*, PCT Patent WO/2007/054505 (2007).
14. Z. H. Luo, X. Z. You and H. R. Li, *Ind. Eng. Chem. Res.*, **48**, 446 (2009).
15. R. Tesser, E. Santacesaria, M. Di Serio, G. Di Nuzzi and V. Fiandra, *Ind. Eng. Chem. Res.*, **46**, 6456 (2007).
16. S. Carrà, E. Santacesarla and M. Morbldlll, *Ind. Eng. Chem. Process Des. Dev.*, **18**, 428 (1979).